

# XYZ States - Results from Experiments

*Sören Lange*

Justus-Liebig-Universität Giessen, II. Physikalisches Institut  
Heinrich-Buff-Ring 16, 35392 Giessen, Germany

June 13, 2021

Lecture given at the  
Helmholtz International Summer School Physics of Heavy Quarks and Hadrons  
Dubna, Russia, 07/15-28/2013.

## 1 Introduction

The static quark anti-quark potential in strong interaction is often expressed using the ansatz

$$\begin{aligned}
 V(r) = & -\frac{4}{3} \frac{\alpha_s}{r} + kr \\
 & + \frac{32\pi\alpha_s}{9m_c^2} \delta(r) \vec{S}_c \vec{S}_{\bar{c}} \\
 & + \frac{1}{m_c^2} \left( \frac{2\alpha_s}{r^3} - \frac{k}{2r} \right) \vec{L} \vec{S} \\
 & + \frac{1}{m_c^2} \frac{4\alpha_s}{r^3} \left( \frac{3\vec{S}_c \vec{r} \cdot \vec{S}_{\bar{c}} \vec{r}}{r^2} - \vec{S}_c \vec{S}_{\bar{c}} \right) .
 \end{aligned} \tag{1}$$

For historic reasons, this potential is referred to as a Cornell-type potential [1] [2] [3]. The first term is a Coulomb-like term describing one-gluon exchange, which is very similar to the Coulomb term in QED potentials for e.g. positronium or the hydrogen atom, except that here the coupling constant is given by  $\alpha_s$  instead of  $\alpha_{em}$ . The second term is a linear term which phenomenologically describes QCD confinement, and which is completely absent in QED. The linear shape is e.g. supported by Lattice QCD calculations, and the parameter  $k$  is the string constant of QCD string between the quark and the anti-quark. The other terms represent spin-orbit, spin-spin and tensor potentials, leading to mass splittings in the spectrum.

Heavy quark combinations such as the charm anti-charm (called charmonium) and the beauty anti-beauty (called bottomonium) are in particular interesting, as they can be treated *(a)* as non-relativistic systems and *(b)* perturbatively due to  $m_Q \gg \Lambda_{QCD}$ , where  $\Lambda_{QCD} \simeq 200$  MeV is the QCD scale.

Charmonium- and bottomonium spectroscopy has been a flourishing field recently, as many new states have been observed. Masses of expected states (such as the  $h_b, h'_b, \eta_b, \eta'_b$ , described below) have been measured accurately and enable precision tests of Eq. 1 to a level of  $\Delta m/m \leq 10^{-4}$ .

On the other hand, several non-expected states were found, which do not fit into the Cornell-type potential model prediction. While for many priorly observed charmonium and bottomonium states the difference between predicted and measured mass is impressively small in the order of  $\Delta m \simeq 2\text{-}3$  MeV, for some of the new states the closest predicted state is off by  $\Delta m \geq 50$  MeV or more. Such states are often referred to as XYZ states. The Z states (as will be described below) are in particular interesting, as they are charged states, and thus can not represent charmonium or bottomonium at all.

Many of the XYZ states were observed at the Belle [4] and BaBar [5] experiments in  $e^+e^-$  collisions at beam energies 10.5-11.0 GeV (i.e. in the  $\Upsilon(nS)$  region). In this draft, at first charmonium-like states will be discussed, which are e.g. produced in  $B$  meson decays. Belle and BABAR are often called  $B$  meson factories, as the number of produced  $B$  mesons per time unit is very high. Often the size of a data sample is given as integrated luminosity. With a typical instantaneous luminosity of  $1 \times 10^{34} \text{ s}^{-1} \text{ cm}^{-2}$  and using  $1 \text{ b ("barn")} = 10^{24} \text{ cm}^2$ , we get  $\simeq 1 \times 10^{-15} \text{ b}^{-1}$  or  $\simeq 1 \text{ fb}^{-1}$  per 1 day. The center-of-mass energy of Belle and BaBar is  $\sqrt{s} = 10.58$  GeV, corresponding to the mass of the  $\Upsilon(4S)$  resonance. The cross section is  $\sigma(e^+e^- \rightarrow \Upsilon(4S)) \simeq 1 \text{ nb}$ , and thus we get about  $1 \times 10^6$  produced  $B$  meson pairs per day.

Further below in this draft, examples for bottomonium-like states will be given, which are e.g. produced in radiative decays of  $\Upsilon(nS)$  resonances. As an example of applications of the measurements, a few precision tests of the Cornell-type potential (Eq. 1) will be discussed. At the end, an outlook to a future experiment will be given, which will be able to measure the width of a state in the sub-MeV regime.

## 2 Charmonium(-like) states

### 2.1 The X(3872) state

The X(3872) state has been discovered in  $B$  meson decay in the decay  $X(3872) \rightarrow J/\psi \pi^+ \pi^-$  by Belle [6] and confirmed by other experiments [7] [8] [9] [10] [11]. Among the XYZ states, the X(3872) is the only one observed in several decay channels:  $X(3872) \rightarrow J/\psi \pi^+ \pi^-$ ,  $X(3872) \rightarrow J/\psi \gamma$ ,  $X(3872) \rightarrow J/\psi \pi^+ \pi^- \pi^0$ ,  $X(3872) \rightarrow D^0 \bar{D}^0 \pi^0$ , and  $X(3872) \rightarrow D^0 \bar{D}^0 \gamma$ .

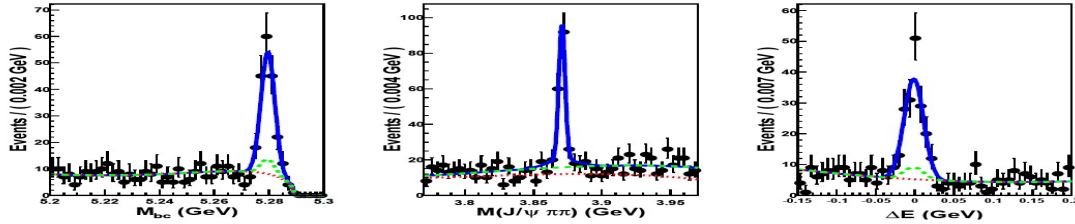


Figure 1: Beam constrained mass  $M_{bc} = \sqrt{(E_{beam}^{cms}/2)^2 - (p_B^{cms})^2}$  (left) invariant mass  $m(J/\psi \pi^+ \pi^-)$  and the energy difference  $\Delta E = E_B^{cms} - E_{beam}^{cms}$  for the decay  $B^+ \rightarrow K^+ X(3872) (\rightarrow J/\psi \pi^+ \pi^-)$ . A 3-dimensional fit is performed. The blue line represents the fit result, which is used to extract the mass and the width of the X(3872).

The mass of the X(3872) can be determined with high precision. A recent mass measurement of the X(3872) at Belle was based upon the complete Belle data set of  $711 \text{ fb}^{-1}$  collected at

the  $\Upsilon(4S)$  resonance. Fig. 1 shows the beam constrained mass  $M_{bc}=\sqrt{(E_{beam}^{cms}/2)^2 - (p_B^{cms})^2}$  (left, with the energy in the center-of-mass system  $E_{beam}^{cms}$  and the momentum of the  $B$  meson in the center-of-mass system  $p_B^{cms}$ ), the invariant mass  $m(J/\psi\pi^+\pi^-)$  (center) and the energy difference  $\Delta E=E_B^{cms}-E_{beam}^{cms}$  (right, with the energy of the  $B$  meson in the center-of-mass system  $E_B^{cms}$ ). Data and fit (as a result of a 3-dimensional fit to the observables shown) for the decay  $B^+\rightarrow K^+X(3872)(\rightarrow J/\psi\pi^+\pi^-)$  are shown (blue line: signal, dashed green line: background). The fitted yield is  $151\pm 15$  events. For details of the analysis procedure see [12]. The fitted mass is listed in Tab. 1 in comparison with mass measurements from other experiments.

The mass measurement reveals the surprising fact that the X(3872) is very close to the  $D^{*0}\bar{D}^0$  threshold. Therefore it was discussed, if the X(3872) possibly represents an  $S$ -wave  $D^{*0}\bar{D}^0$  molecular state [13]. In this case, the binding energy  $E_b$  would be given by the mass difference  $m(X)-m(D^{*0})-m(D^0)$ . Including the new Belle result, the new world average mass of the X(3872) is  $m=3871.68\pm 0.17$  MeV [14]. The present value for the sum of the masses is  $m(D^0)+m(D^{*0})=3871.84\pm 0.28$  MeV [14], Thus, a binding energy of  $E_b=-0.16\pm 0.33$  MeV can be calculated, which is enormously small. In addition,  $E_b$  is inverse proportional to the squared scattering length  $a$  [15]:

$$E_b = \frac{\hbar^2}{2\mu a^2} \quad (2)$$

using the reduced mass  $\mu$ . The radius can in first order be approximated by  $\langle r \rangle = a/\sqrt{2}$ . This would surprisingly mean a very large radius  $\langle r \rangle \geq 10_{-5}^{+\infty}$  fm of the molecular state.

Experiment	Mass of X(3872)	
CDF2	$3871.61\pm 0.16\pm 0.19$ MeV	[8]
BaBar ( $B^+$ )	$3871.4\pm 0.6\pm 0.1$ MeV	[7]
BaBar ( $B^0$ )	$3868.7\pm 1.5\pm 0.4$ MeV	[7]
D0	$3871.8\pm 3.1\pm 3.0$ MeV	[9]
Belle	$3871.84\pm 0.27\pm 0.19$ MeV	[12]
LHCb	$3871.95\pm 0.48\pm 0.12$ MeV	[10]
New World Average	$3871.68\pm 0.17$ MeV	[14]

Table 1: Mass measurements of the X(3872).

An important decay of the X(3872) is the radiative decay  $X(3872)\rightarrow J/\psi\gamma$ . The observation of this decay was reported by Belle with a data set of  $256 fb^{-1}$ , a yield of  $13.6\pm 4.4$  events and a statistical significance of  $4.0\sigma$  [16]. The combined branching ratio was measured to  $BR(B^\pm\rightarrow XK^\pm, X\rightarrow\gamma J/\psi) = (1.8\pm 0.6\pm 0.1)\times 10^{-6}$ , i.e. the branching fraction of  $X(3872)\rightarrow J/\psi\gamma$  is a factor  $\simeq 6$  smaller than the one for  $X(3872)\rightarrow J/\psi\pi^+\pi^-$ , and thus this decay represents a rare decay. However, the decay is very important, as it represents a decay into two neutral particles, which are identical to their anti-particles. Therefore observation of the decay implies, that the charge conjugation of the X(3872) must be  $C=+1$ . BABAR was able to confirm the observation with a data set of  $260 fb^{-1}$ , a yield of  $19.4\pm 5.7$  events and a statistical significance of  $3.4\sigma$  [17]. Charmonium states with  $C=+1$  are interesting objects. While decay widths (which can be measured by branching fractions in the experiment) for  $C=-1$  states scale

with the squared modulus of the wave function ( $\Gamma \sim |\Psi(r=0)|^2$ ), decay widths of  $C=+1$  states scale with the squared modulus of the *derivative* of the wave function ( $\Gamma \sim |\partial\Psi/\partial r(r=0)|^2$ ). An additional surprising property of the  $X(3872)$  is isospin violation. It was found, that in the decay  $X(3872) \rightarrow J/\psi \pi^+ \pi^-$  the invariant mass peaks at the mass of the  $\rho^0$  meson. The  $\rho^0$  carries isospin  $I=0$ , but the initial state (if assumed to be a pure  $c\bar{c}$  state) has  $I=0$  (as it would not contain any  $u$  or  $d$  valence quarks). There are only two additional isospin violating transitions known in the charmonium system [14], namely  $\psi' \rightarrow J/\psi \pi^0$  ( $\mathcal{B}=1.3 \pm 0.1 \cdot 10^{-3}$ ) and  $\psi' \rightarrow h_c \pi^0$  ( $\mathcal{B}=8.4 \pm 1.6 \cdot 10^{-4}$ ). These branching fractions are very small. One of the mechanisms to induce isospin violation is the  $u/d$  quark mass difference in strong interaction. However, as the mass difference is small, the effect should be very small, consistent with the measured branching fractions. Another possible mechanism to induce isospin violation is the  $u/d$  quark charge difference in electromagnetic interactions (EM). Isospin should only be conserved in strong interaction, but not in EM interaction. Thus one of the possible explanations might be, that the decay  $X(3872) \rightarrow J/\psi \rho(\rightarrow \pi^+ \pi^-)$  is proceeding via EM interaction, i.e. the  $\rho$  might not be created by two gluons, but by a virtual photon. However, then the decay should be suppressed by an additional factor  $\alpha_{em}/\alpha_S \simeq 10$ . The observation for the  $X(3872)$  is different: the branching fraction of isospin violating transition is (among the known decays) order of  $O(10\%)$  and thus seems to be largely enhanced.

## 2.2 The $Y(4260)$ family

	BaBar [18]	CLEO-c [19]	Belle [20]	Belle [21]	BaBar [22]	BaBar [23]
$\mathcal{L}$	$211 \text{ fb}^{-1}$	$13.3 \text{ fb}^{-1}$	$553 \text{ fb}^{-1}$	$548 \text{ fb}^{-1}$	$454 \text{ fb}^{-1}$	$454 \text{ fb}^{-1}$
N	$125 \pm 23$	$14.1^{+5.2}_{-4.2}$	$165 \pm 24$	$324 \pm 21$	$344 \pm 39$	–
Significance	$\simeq 8\sigma$	$\simeq 4.9\sigma$	$\geq 7\sigma$	$\geq 15\sigma$	–	–
$m / \text{MeV}$	$4259 \pm 8^{+2}_{-6}$	$4283^{+17}_{-16} \pm 4$	$4295 \pm 10^{+10}_{-3}$	$4247 \pm 12^{+17}_{-32}$	$4252 \pm 6^{+2}_{-3}$	$4244 \pm 5 \pm 4$
$\Gamma / \text{MeV}$	$88 \pm 23^{+6}_{-4}$	$70^{+40}_{-25}$	$133 \pm 26^{+13}_{-6}$	$108 \pm 19 \pm 10$	$105 \pm 18^{+4}_{-6}$	$114^{+16}_{-15} \pm 7$

Table 2: Summary of the mass and width measurements of the  $Y(4260)$ .

Another new charmonium-like state was observed by *BABAR* and confirmed by several experiments (see Tab. 2 for a list of the measured masses and widths) at a high mass of  $m \simeq 4260$  MeV, far above the  $D\bar{D}$  threshold. The width is  $\leq 100$  MeV, which is quite narrow for such a high state. The observed decay is again a  $\pi^+ \pi^-$  transition to the  $J/\psi$ , similar to the above mentioned decay of the  $X(3872)$ . However, the production mechanism is not  $B$  meson decay but instead ISR (initial state radiation), i.e.  $e^+ e^- \rightarrow \gamma_{ISR} Y(4260)$ , i.e. a photon is radiated by either the  $e^+$  or the  $e^-$  in the initial state, lowering the  $\sqrt{s}$  and producing the  $Y(4260)$  by a virtual photon. In fact, not only one state, but four states have been observed and are shown in Fig. 2, i.e. the  $Y(4008)$ , the  $Y(4260)$ , the  $Y(4250)$  and the  $Y(4660)$ . In a search by Belle no additional state up to  $m \leq 7$  GeV was found. All the  $Y$  states must have the quantum numbers  $J^{PC}=1^{--}$ , due to the observation in an initial state radiation process. As an intriguing fact, there are known and assigned  $J^P=1^{--}$  charmonium states:  $J/\psi$ ,  $\psi(2S)$ ,  $\psi(4040)$ ,  $\psi(4160)$  and  $\psi(4415)$ . Thus, there is a clear over-population of  $1^{--}$  states in the  $m \geq 4$  GeV region. Despite partial overlap, apparently there seems to be no mixing: (a) no mixing among them, i.e. the  $Y(4008)$  and the  $Y(4260)$  decay to  $J/\psi \pi^+ \pi^-$ , and the  $Y(4350)$  and the  $Y(4660)$  decay to  $\psi' \pi^+ \pi^-$ , and neither of one has been observed in the other channel, and (b) no mixing with  $\psi$  states with



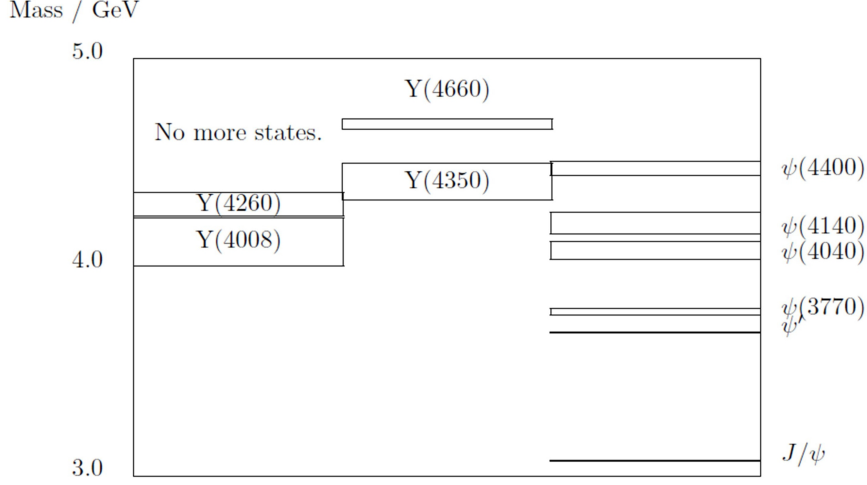


Figure 3: Level scheme for  $J^{PC}=1^{--}$  states: states decaying into  $J/\psi\pi^+\pi^-$  (left column), states decaying into  $\psi'\pi^+\pi^-$  (center column), and known  $\psi$  states (radial quantum number  $n=1,\dots,6$ ).

the signal was observed in  $e^+e^- \rightarrow \gamma_{ISR} \Lambda_c^+ \Lambda_c^-$ . The state is usually referred to as X(4630). The  $\Lambda_c^+$  is reconstructed in the final states  $pK_s^0(\rightarrow\pi^+\pi^-)$ ,  $pK^-\pi^+$  and  $\Lambda(\rightarrow p\pi^-)\pi^+$ . For the  $\Lambda_c^-$  only partial reconstruction is used: The recoil mass to  $[\Lambda_c^+\gamma]$  is investigated while requiring an anti-proton (from the  $\Lambda_c^-$  decay) as a tag and then a cut around the  $\Lambda_c^-$  mass is applied. The measured mass is  $m=4634_{-7-8}^{+8+5}$  MeV and the measured width  $\Gamma=92_{-24-21}^{+40+10}$  MeV. Fig. 4 shows the invariant mass  $m(\Lambda_c^+\Lambda_c^-)$ . A signal with a statistical significance of  $8.2\sigma$  is observed. The observation of this state is remarkable because of two reasons:

- It is the highest charmonium state observed so far (together with the Y(4660) of almost same mass, but decaying into  $J/\psi\pi^+\pi^-$ ), and
- the only new state so far observed to decay into baryons.

The potential model has an important boundary condition for the radial wave function, which is called the turning point  $R_{tp}$  and can be calculated as

$$R_{tp} = \frac{E - 2m}{2\sigma} + \sqrt{\frac{4m^2 - 4mE + E^2}{4\sigma^2} + \frac{4\alpha_S}{3\sigma}} \quad (3)$$

using  $\sigma=\hbar ck$  with the string constant  $k$ . This is the radius, at which (a) the Wronski determinant must be zero and (b) the radial wave function changes into an asymptotic, exponential tail. For a box potential, the turning point would be identical to  $r_{box}$ , and the exponential tail of the wave function would be outside the box. Fig. 5 shows the turning point radius as a function of the mass. For the X(4630), if it is a charmonium state, the turning point is at  $r_{turningpoint} > 2.1$  fm. However, a radius of  $r \approx 1.25$  fm marks the QCD string breaking regime. Thus, if the Y(4660) or the X(4630) are charmonium states, it is unclear, how such a large part of the wave function of a bound state can be in the string breaking regime. In any case, if it is a charmonium state, the radial quantum number must be  $n \geq 4$ .

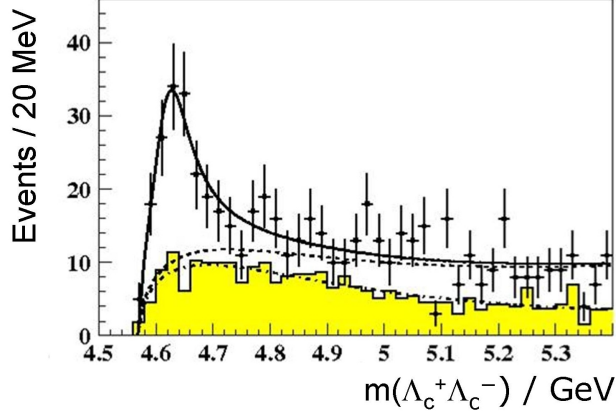


Figure 4: Invariant mass  $m(\Lambda_c^+\Lambda_c^-)$  for the process  $e^+e^- \rightarrow \gamma_{ISR}\Lambda_c^+\Lambda_c^-$  at Belle [28] showing the signal for the X(4630).

## 2.4 The $Z_c(3900)$ state

A new state, tentatively called the  $Z_c^+(3900)$ , was observed by BESIII [29] in the decay of the  $Y(4260) \rightarrow Z_c^+(3900)\pi^\pm$  in a data set of  $525 \text{ pb}^{-1}$ . BESIII is operating with center-of-mass energies in the charmonium mass region, and producing the  $Y(4260)$  directly via  $e^+e^- \rightarrow Y(4260)$  at  $\sqrt{s}=4.26 \text{ GeV}$ . Importantly the  $Z_c^+(3900)$  is a charged state, and thus can not be a charmonium state. A charged combination could be formed by a state composed of four quarks. This may be tetraquark state (such as  $[cu\bar{c}\bar{d}]$ ) or a molecular state (such as  $D^\pm \bar{D}^{0*}$ ). The  $Z_c^+(3900)$  was reconstructed in the decay to  $J/\psi\pi^\mp$ . Fig. 6 (left) shows the observed signal, which has a statistical significance of  $>8\sigma$ . From the two charged pions, the one is used, which gives the higher invariant mass for  $J/\psi\pi^\pm$ , in order to remove combinatorial background from the charged pion of the  $Y(4260)$  transition to the new state. The measured mass is  $m=3899.0 \pm 3.6 \pm 4.9 \text{ MeV}$  and the measured width  $\Gamma=46 \pm 10 \pm 20 \text{ MeV}$ . The observation of this new state is remarkable because this state seems to provide for the first time a connection between the Z states and the Y states, possibly pointing to the same interpretation of their nature. Only a few days later, the state was confirmed by Belle [30] in the same decay channel  $J/\psi\pi^\mp$  and also in  $Y(4260)$  decays, while in the Belle case the  $Y(4260)$  was produced in the ISR process  $\Upsilon(nS) \rightarrow \gamma_{ISR}Y(4260)$ . The measure mass of  $m=3894.5 \pm 6.6 \pm 4.5 \text{ MeV}$  and width  $\Gamma=63 \pm 24 \pm 26 \text{ MeV}$  are both consistent with the BESIII measurement. Fig. 6 (right) shows the observed signal, which has a statistical significance of  $>8\sigma$  in a data set of  $967 \text{ fb}^{-1}$ . Again, as the  $Z_c^+(4430)$ , the state was observed as  $Z_c^+(3900)$  and  $Z_c^-(3900)$  with about the same yield [29], indicating a doublet. Concerning the quantum numbers, remarkably the isospin must be  $I=1$ , (as the isospin of the pion is  $I=1$ ), if we assume  $I=0$  for the  $Y(4260)$ . If the heavy meson pair is assumed to be in the  $S$ -wave, the spin-parity of the state is uniquely determined as  $J^P=1^+$ .  $C$ -parity  $(-1)^{L+S}$  is only defined for neutral particles, thus there can only be a  $G$ -parity assignment to the  $Z_c^+(3900)$ . The  $G$ -parity  $(-1)^{L+S+I}$  with  $L=0$ ,  $S=1$  and  $I=1$  thus gives  $G=+$ . As  $G$ -parity should be preserved in strong decays, this assignment, due to the  $G$ -parity  $G=-$  for the pion, has the interesting implication that the  $Y(4260)$  would have  $G=-$ . This would be compatible with an

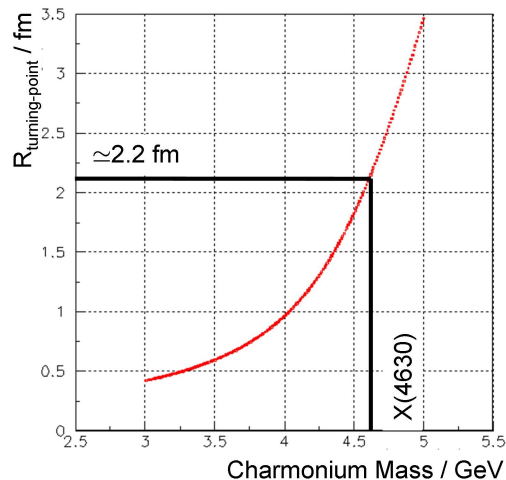


Figure 5: Radius of the turning point of a  $c\bar{c}$  wave function in the Cornell potential vs. the charmonium mass.

$I=0$  isosinglet assignment for the  $Y(4260)$ , which has the important implication, that there is no charged partner of the  $Y(4260)$  existing.

## 2.5 A $D$ -wave state

Belle investigated the decay  $B^+ \rightarrow K^+ \chi_{c1} \gamma$  with  $\chi_{c1} \rightarrow J/\psi \gamma$  using a data set of  $711 \text{ fb}^{-1}$  [31]. A search for charmonium(-like) states decaying to  $\chi_{c1} \gamma$  was performed. Fig. 7 shows the invariant mass  $m(\chi_{c1} \gamma)$ . In other words, the search was based upon a sequence of two radiative decays with both  $\Delta L=1$ . The radiative transition also flips the parity due to the quantum numbers of the photon  $J^P=1^-$ , and therefore the requirement of the intermediate  $\chi_{c1}$  with positive parity. A new state at a mass of  $3823.1 \pm 1.8 \pm 0.7 \text{ MeV}$  was observed with a  $3.8\sigma$  significance. The product branching fraction was measured as  $\mathcal{B}(B^+ \rightarrow K^+ X(3820)) \times \mathcal{B}(X(3820) \rightarrow \chi_{c1} \gamma) = (9.7^{+2.8+1.1}_{-2.5-1.0}) \times 10^4$ , which is a factor  $\simeq 10$  larger than e.g. the sum of all measured product branching fractions of the  $X(3872)$ . The observed state might be one of the charmonium  $D$ -wave ( $L=2$ ) states, as such states should primarily decay radiatively to  $\chi_{cJ}$  states by  $L=2 \rightarrow L=1$  transitions and according branching fractions should be high  $\geq 50\%$  [32] [33]. There are four expected  $n=1$   $D$ -wave states: the  $\eta_{c2}$  ( $^1D_2$ ) with  $J^{PC}=2^{-+}$  and  $\psi_{1,2,3}$  ( $^3D_{1,2,3}$ ) with  $J^{PC}=1,2,3^{--}$ . The prediction [3] for the  $\psi_1$  ( $^3D_1$ ) of  $3.7699 \text{ GeV}$  is much lower than the observed  $X(3820)$ . The  $\psi_3$  ( $^3D_3$ ) can not decay radiatively by an E1 transition and should thus be suppressed. The  $\eta_{c2}$  ( $^1D_2$ ) would require a spin-flip in the transition, and should be suppressed as well. The only candidate, which fulfills all the required properties, is the  $\psi_2$  ( $^3D_2$ ) state with  $J^{PC}=2^{--}$  and a predicted mass  $3.838 \text{ MeV}$  [3], which is close to the observed mass. In addition, the  $\psi_2$  is predicted to be narrow  $\Gamma \simeq 300\text{-}400 \text{ keV}$  [32], consistent with a preliminary measured width  $\Gamma = 4 \pm 6 \text{ MeV}$ . As the observed state is above the open charm thresholds ( $3730 \text{ MeV}$  for  $D^0 \bar{D}^0$  and  $3739 \text{ MeV}$  for  $D^+ D^-$ , respectively), decays into final states with charm should be expected. However, for the  $\psi_2$  the decay  $2^{--} \rightarrow 0^{-+} 0^{-+}$  with  $\Delta L=2$  (i.e.  $(-1)^L = +1$ ) is forbidden

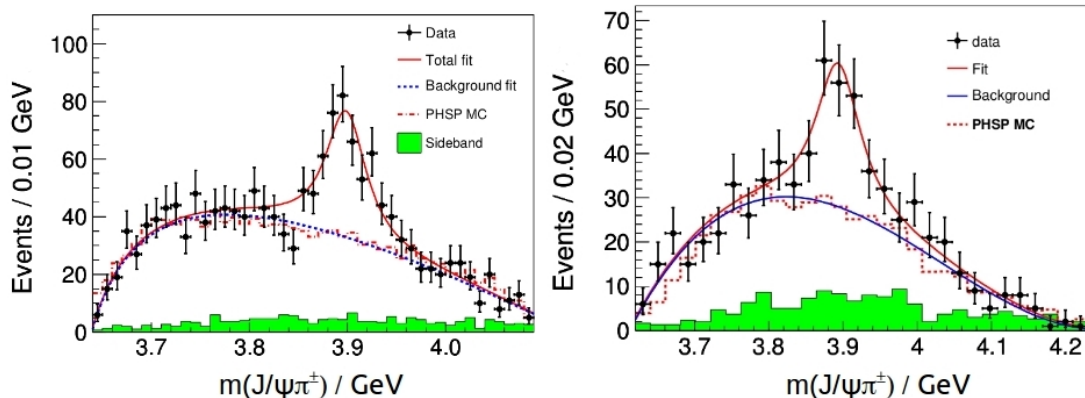


Figure 6:  $J/\psi\pi\pi^\mp$  invariant mass in  $Y(4260)$  decays, indicating the  $Z_c^+(3900)$  signal for BESIII (left) [29] and Belle (right) [30]. For details see text.

by parity conservation, and thus other decays (such as the observed one) should be enhanced. This mechanism could explain the high observed branching fraction into  $J/\psi\gamma\gamma$ . Note that the decays to  $D\bar{D}^*$  or  $D^*\bar{D}$  are forbidden by energy conservation. The observed product branching fraction is consistent with a calculation with color-octet amplitudes [34] predicting  $\mathcal{B}(B \rightarrow K^3 D_2) \times \mathcal{B}(^3 D_2 \rightarrow \chi_{c1} \gamma) = (3.7 - 7.5) \times 10^{-4}$ .

### 3 Bottomonium(-like) states

#### 3.1 The $h_b(1P)$ and the $h_b(2P)$

In a recent analysis by Belle, a particular technique was used, namely the study of *missing mass* to a  $\pi^+\pi^-$  pairs in  $\Upsilon(5S)$  decays [35]. Fig. 8 shows the background-subtracted missing mass for a  $\Upsilon(5S)$  data set of  $121.4 \text{ fb}^{-1}$ . Among several known states such as the  $\Upsilon(1S)$ ,  $\Upsilon(2S)$ ,  $\Upsilon(3S)$  and  $\Upsilon(1D)$ , there are additional peaks arising from the transitions  $\Upsilon(3S) \rightarrow \Upsilon(1S)\pi^+\pi^-$ ,  $\Upsilon(2S) \rightarrow \Upsilon(1S)\pi^+\pi^-$ , with the  $\Upsilon(3S)$  and  $\Upsilon(2S)$  being produced in the decay of the primary  $\Upsilon(5S)$ . In addition to the expected signals, first observations of the bottomonium singlet  $P$ -wave states  $h_b(1P)$  and  $h_b(2P)$  were made. Their measured masses are  $m = 9898.3 \pm 1.1_{-1.1}^{+1.0} \text{ MeV}$  and  $m = 10259.8 \pm 0.6_{-1.0}^{+1.4} \text{ MeV}$ , respectively. The red, dashed lines in Fig. 8 indicate regions of different paramtrisations of the background. For the  $h_b$ , this measurement is consistent with the first evidence ( $3.1\sigma$  stat. significance) by BaBar in  $\Upsilon(3S)$  decays with a mass of  $9902 \pm 4(\text{stat.}) \pm 2(\text{syst.}) \text{ MeV}$  [36]. The masses can be compared to predictions from potential model calculations [37] with 9901 MeV and 10261 MeV, respectively, i.e. the deviations are only 2.7 MeV and 1.2 MeV.

#### 3.2 The $\eta_b(1S)$ and the $\eta_b(2S)$

The  $\eta_b(1S)$  is the bottomonium ground state  $1^1S_0$  with  $J^{PC} = 0^{-+}$ . It was discovered by BaBar in the radiative decay  $\Upsilon(3S) \rightarrow \gamma\eta_b$ . The measured mass was  $9388.9_{-2.3}^{+3.1}(\text{stat}) \pm 2.7(\text{syst}) \text{ MeV}$ ,

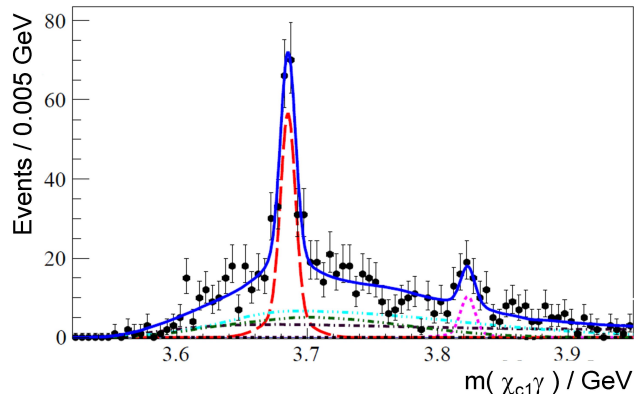


Figure 7: Invariant mass  $m(\chi_{c1}\gamma)$  in  $B$  meson decays at Belle [31] showing the signal of the  $^3D_2$  charmonium candidate X(3820). The dashed, dotted and dash-dotted line represent different backgrounds (combinatorial, peaking and non-peaking background from  $\psi'$  and X(3872) decays other than  $\chi_{cJ}\gamma$ , respectively, where the term peaking refers to peaking in  $m_{BC}$ ).

The observation was confirmed by CLEO III using 6 million Upsilon(3S) decays with a measured mass  $m=9391.8\pm 6.6\pm 2.0$  MeV. The observation of the  $h_b$  (see above) by Belle also enabled a search for the radiative decay  $h_b(1P)\rightarrow\eta_b(1S)\gamma$ , which was observed with a very high significance  $>13\sigma$  in a dataset of  $133.4\text{ fb}^{-1}$  at the  $\Upsilon(5S)$  and in the nearby continuum [38]. In addition, even the  $\eta_b(2S)$  was observed in  $h_b(2P)\rightarrow\eta_b(2S)\gamma$ . Fig. 9 shows the  $\pi^+\pi^-\gamma$  missing mass for the case of the  $\eta_b(1S)$  (left) and  $\eta_b(2S)$  (right), where the charged pion pair originates from the transition  $\Upsilon(5S)\rightarrow h_b(1P,2P)\pi^+\pi^-$ . The measured masses are  $m(\eta_b(1S))=9402.4\pm 1.5\pm 1.8$  MeV and  $m(\eta_b(2S))=9999.0\pm 3.5_{-1.9}^{+2.8}$  MeV. Due to the high resolution, this measurement also enabled the measurement of the width of the  $\eta_b$  as  $\Gamma=10.8_{-3.7-2.0}^{+4.0+4.5}$ , which is consistent with the expectation from potential models to  $5\leq\Gamma\leq 20$  MeV. The measurements of the  $\eta_b(1S)$  and  $\eta_b(2S)$  allow precision determination of the hyperfine mass splittings  $\Upsilon(1S)-\eta_b(1S)$  and  $\Upsilon(2S)-\eta_b(2S)$ , using the masses of the  $\Upsilon(1S)$  and  $\Upsilon(2S)$  from [14]. The mass splittings are listed in Tab. 3. The splittings are in good agreement with the expectation from a potential model with relativistic corrections [37] or lattice QCD calculations with kinetic terms up to  $O(v^6)$  [39]. However, lattice QCD calculations to  $O(v^4)$  with charm sea quarks predict higher splittings which are  $\simeq 10$  MeV larger. Note that perturbative non-relativistic QCD calculations up to order  $(m_b\alpha_S)^5$  predict significant smaller splittings e.g.  $39\pm 11_{-8}^{+9}$  MeV [40].

## 4 Test of the tensor term in the potential

The measured masses of the  $h_b$  and  $h'_b$  can be used for a precision test of the hyperfine splitting in the Cornell-type potential (Eq. 1), i.e. a test of the relation

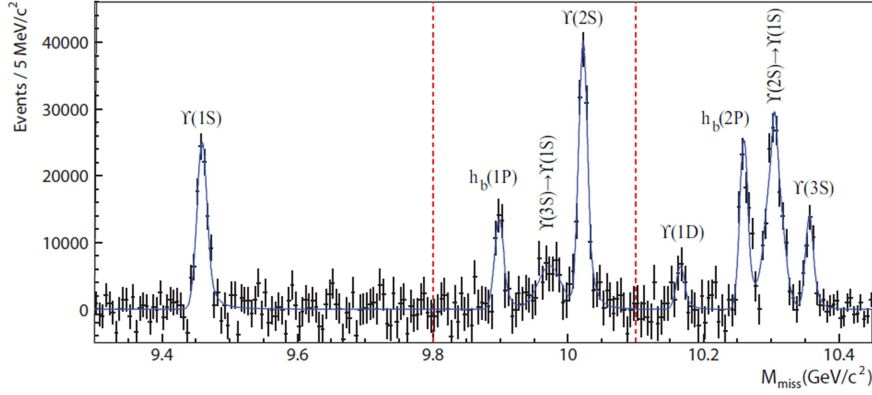


Figure 8: Observation of the  $h_b(1S)$  and  $h_b(2S)$  at Belle. For details see text.

	Belle [38]	Potential [37]	LQCD [41]	LQCD [39]
$\Upsilon(1S)-\eta_b$	$57.9\pm 2.3$ MeV	60.0	$70\pm 9$ MeV	$60.3\pm 5.5\pm 5.0\pm 2.1$ MeV
$\Upsilon(2S)-\eta'_b$	$24.3^{+4.0}_{-4.5}$ MeV	30.0	$35\pm 3$ MeV	$23.5\pm 4.1\pm 2.1\pm 0.8$ MeV

Table 3: Bottomonium hyperfine splittings: measurement, calculated by potential model and calculated by Lattice QCD (LQCD).

$$m(h_b) \stackrel{?}{=} \frac{m(\chi_{b0}) + 3 \cdot m(\chi_{b1}) + 5 \cdot m(\chi_{b2})}{9} \quad (4)$$

using the world average masses of the  $\chi_{b0,1,2}$  and  $\chi'_{b0,1,2}$  from [14]. The hyperfine splitting  $\Delta m_{HF} = m(n^3P_J) - m(n^1P_1)$  was measured as  $\Delta m_{HF} = (+1.6 \pm 1.5)$  MeV for  $n=1$  and  $\Delta m_{HF} = (+0.5^{+1.6}_{-1.2})$  MeV for  $n=2$ . This can be used as a test for the tensor term in the potential

$$V_{tensor} = \frac{1}{m^2} \frac{4\alpha_S}{r^3} \left( \frac{3\vec{S}_1\vec{r} \cdot \vec{S}_2\vec{r}}{r^2} - \vec{S}_1\vec{S}_2 \right) \quad (5)$$

with the spins of the heavy quarks  $\vec{S}_1$  and  $\vec{S}_2$ , the heavy quark mass  $m$  and the quark antiquark distance  $r$ , which is usually treated as a perturbation in the potential. It vanishes for  $S=0$  (e.g.  $\eta_b$ ,  $\Upsilon(nS)$ ,  $h_b$ , ...) and  $L=0$  (e.g.  $^1D_2$  state, ...). In a simplified view, a non-zero  $\Delta m_{HF}$  would mean, that the wavefunction of the  $h_b$  at  $r=0$  is non-vanishing. The sign of the potential term is positive, thus masses should be shifted up. Although the above mentioned measurements of  $\Delta m_{HF}$  are consistent with zero, however positive values seem to be preferred for the  $b\bar{b}$  case, mildly suggesting to indicate an effect of the tensor term. This can be compared to measurements of  $\Delta m_{HF} = 0.02 \pm 0.19 \pm 0.13$  MeV [42] and  $\Delta m_{HF} = 0.10 \pm 0.13 \pm 0.18$  MeV [43] charmonium system, (i.e. the  $h_c$ ).

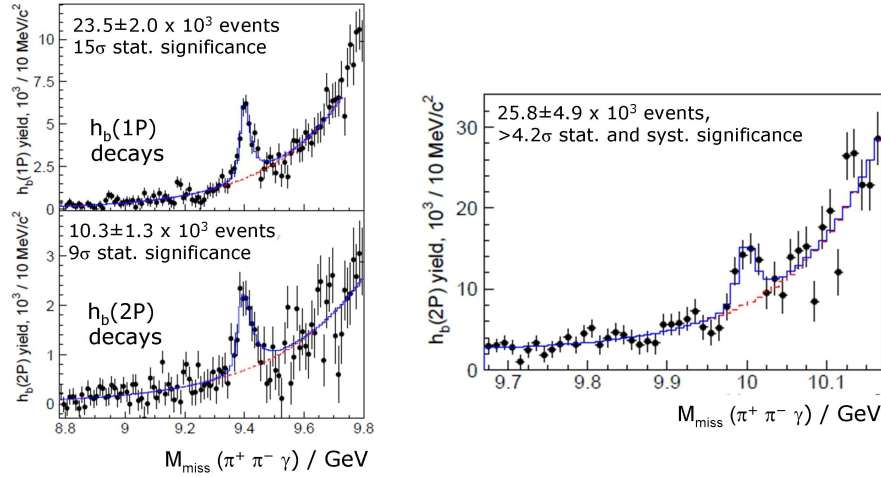


Figure 9: Observations of the  $\eta_b(1P)$  (left) and  $\eta_b(2P)$  (right) at Belle. For details see text.

#### 4.1 Test of flavor independence of the potential

The new mass measurements in the bottomonium region enable for the first time a precision test of the flavour independance of the  $c\bar{c}$  and  $b\bar{b}$  systems. The important question is, if the level spacing is independant from the quark mass. According to [44], for a potential of the form  $V(r)=\lambda r^\nu$  the level spacing is  $\Delta E \propto (2\mu/\hbar^2)^{-\nu/(2+\nu)} |\lambda|^{2/(2+\nu)}$ . where  $\mu$  is the (reduced) quark mass. For a pure Coulomb potential ( $\nu=-1$ ), which should be dominating for the low lying states, this leads to  $\Delta E \propto \mu$ . This would imply that the level spacing would increase linearly with mass, i.e.  $\Delta E(b\bar{b}) \simeq 3\Delta E(c\bar{c})$ . For a pure linear potential it would be  $\Delta E \propto \mu^{-1/3}$ , thus the level spacing would decrease for higher quark masses, i.e.  $\Delta E(b\bar{b}) \simeq 0.5\Delta E(c\bar{c})$ . As can be seen in Fig. 10, for the mass splittings involving the  $h_b$  ( $S=0, L=1$ ) the agreement between  $c\bar{c}$  and  $b\bar{b}$  is excellent, i.e. 10.2 vs. 10.1 MeV and 43.9 vs. 43.8 MeV. There are two possible explanations of this remarkable symmetry. (1) For a pure logarithmic potential  $V(r)=\lambda \ln r$  (i.e. the limit  $\nu \rightarrow 0$ ) the level spacing is  $\Delta E \propto \lambda \mu^0$ . This means, the flavour independance would be strictly fulfilled. (2) The other way to reach the flavour independance is, that the Coulomb potential with  $\Delta E(b\bar{b}) \simeq 3\Delta E(c\bar{c})$  (see above) and the linear potential with  $\Delta E(b\bar{b}) \simeq 0.5\Delta E(c\bar{c})$  (see above) cancel each other quantitatively in an exact way. It also implies that the size of the according  $\lambda$  pre-factors ( $\lambda = -4/3\alpha_S$  for the Coulomb-like potential and  $\lambda = k$  for the linear potential) just seem to have the exactly correct size assigned by nature in a fundamental way. For the ground states ( $S=0, L=0$ ) the agreement of the mass splittings between  $c\bar{c}$  and  $b\bar{b}$  is not as good, i.e. 65.7 vs. 59.7 MeV, and may point to the fact, that there is an additional effect which lowers the  $\eta_c$  mass. This might be mixing of the  $\eta_c$  with the light quark states of the same quantum number  $0^{-+}$  (i.e.  $\eta$  or  $\eta'$ ).

#### 4.2 The $Y_b(10889)$ state

While investigating  $\Upsilon(5S)$  decays, Belle discovered a highly anomalous behavior. For the  $\Upsilon(5S)$ , the beam energies of the KEK-B accelerator were changed in a way, to keep the center-of-mass boost the same as on the  $\Upsilon(4S)$  resonance. Thus, all analysis techniques could be applied. In

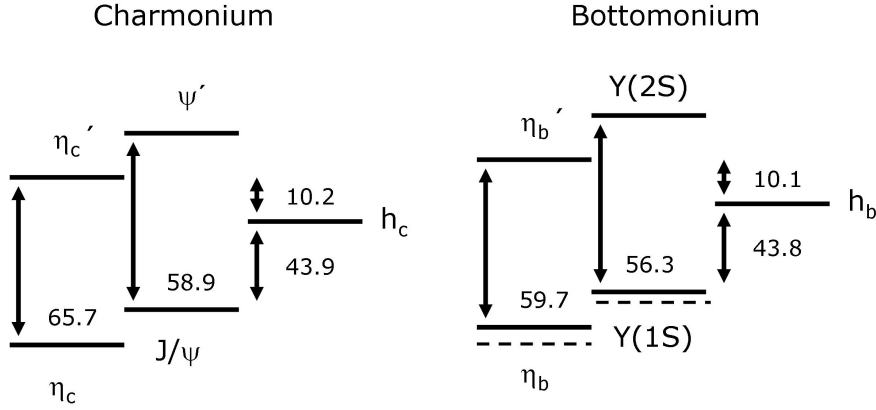


Figure 10: Mass splittings (in MeV) based upon the new measurements [38] of the  $h_b$ ,  $\eta_b$  and  $\eta_b'$ , using masses from [14] for the other states, for charmonium (left) and bottomonium (right). The dotted lines indicate levels for the theoretical case of exact flavour independence.

a data set of  $21.7 \text{ fb}^{-1}$ , the processes  $e^+e^- \rightarrow \Upsilon(nS)\pi^+\pi^-$  with  $n=1,2,3$  were investigated. First of all, the cross section of decays to the  $\Upsilon(1S)$  was found to be anomalously large. While in a data set of  $477 \text{ fb}^{-1}$  on the  $\Upsilon(4S)$ ,  $N=44\pm 8$  events of  $\Upsilon(1S)\pi^+\pi^-$  were observed [45], in the data set of  $21.7 \text{ fb}^{-1}$  on the  $\Upsilon(5S)$   $N=325\pm 20$  events of  $\Upsilon(1S)\pi^+\pi^-$  were observed [46]. This means, that in a data set corresponding to  $\simeq 1/20$  the size of the data set and  $\simeq 1/10$  of the production cross section, still a factor 7.4 more events are observed. This corresponds in total to a signal, which is more than a factor  $10^3$  higher than the expectation. In addition, not only the  $\Upsilon(5S) \rightarrow \Upsilon(1S)\pi^+\pi^-$  but also the  $\Upsilon(5S) \rightarrow \Upsilon(2S)\pi^+\pi^-$  was found to be larger than expected by more than a factor  $5 \times 10^2$ . Note that  $\Upsilon(5S) \rightarrow \Upsilon(4S)\pi^+\pi^-$  is kinematically suppressed. One of the possible explanation for the observed anomalously high yield was a new resonance nearby the  $\Upsilon(5S)$ , decaying into the same final state [47]. Therefore a beam energy scan was performed [48]. Typical step sizes in the variation of the  $\sqrt{s}$  were 6-10 MeV. On each scan point more than  $30 \text{ pb}^{-1}$  were performed. For each energy point, the yield of  $\Upsilon(1S,2S,3S)\pi^+\pi^-$  was determined by an unbinned maximum likelihood fit.

Fig. 11 (bottom) shows the fitted signal yield as a function of  $\sqrt{s}$ . These excitation curves are fitted with a Breit-Wigner shape with floating mean and width, but constraint to be identical parameters for all three curves. The normalizations for the three curves are floating independently. The fitted mean is at  $\simeq 20 \text{ MeV}$  higher mass and the width is about a factor  $\simeq 2$  narrower than the  $\Upsilon(5S)$ . This indicates that the observed resonance is not the  $\Upsilon(5S)$ , but instead a new state which was given the name  $Y_b(10889)$ .

For comparison, Fig. 11 (top) shows the ratio  $R_b$  vs.  $\sqrt{s}$ , where  $R_b$  is defined as the ratio of the inclusive hadronic cross section  $\sigma(e^+e^- \rightarrow \text{hadrons})$  to  $\sigma(e^+e^- \rightarrow \mu^+\mu^-)$ . The final measurement for the new state yields a mass of  $m=10888.4_{-2.6}^{+2.7} \pm 1.2 \text{ MeV}$  and a width of  $\Gamma=30.7_{-7.0}^{+8.3} \pm 3.1 \text{ MeV}$ . The final results for the widths, as measured in the resonance scan, are summarized in Tab. 4. As the  $Y_b(10889)$  does not coincide with a threshold, it cannot be interpreted as a molecule, neither as a threshold effect. there must be another explanation for its nature. The lowest lying tetraquark state with  $J^{PC}=1^{--}$  is predicted at a mass  $m=10.890 \text{ MeV}$  [49], well consistent with the experimental observation. It would be a  $[bq\bar{b}\bar{q}]$  tetraquark, where  $q$  denotes

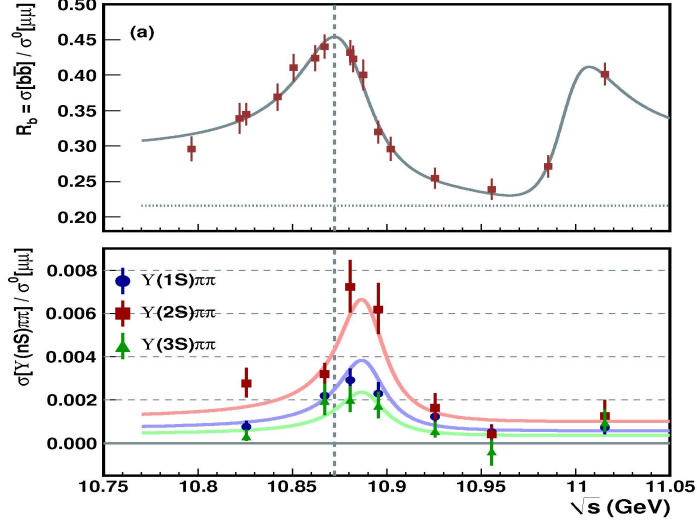


Figure 11:  $R_b$  as a function of  $\sqrt{s}$  (top) and the energy-dependent cross sections for  $e^+e^- \rightarrow \Upsilon(nS)\pi^+\pi^-$  ( $n = 1, 2, 3$ ) processes (bottom). The results of the fits are shown as smooth curves. The vertical dashed line indicates the mass of the  $\Upsilon(5S)$ , as determined from the fit in the upper plot (i.e. the measured location of the maximum hadronic cross section).

a light  $u$  or  $d$  quark, which are assumed to have the identical constituent mass of 305 MeV. In addition, the tetraquark model could explain the observed anomalous yield [49], . If the  $Y_b(10889)$  is a pure  $b\bar{b}$  state, there are no light quarks in the initial state. The  $\pi^+\pi^-$  pair in the  $\Upsilon(5S) \rightarrow \Upsilon(1S, 2S, 3S)\pi^+\pi^-$  transition must be created by two gluons and subsequent  $g \rightarrow u\bar{u}$ ,  $g \rightarrow d\bar{d}$ , and rearrangement to  $u\bar{d}$  and  $d\bar{u}$ . Thus, the transition would be Zweig forbidden. If the  $Y_b(10889)$  is a  $[bq][\bar{b}\bar{q}]$  tetraquark, then there is a  $u\bar{u}$  or  $d\bar{d}$  already present in the initial state, and only one additional pair must be formed from the QCD vacuum. Thus, the transition is Zweig allowed and the transition rate would be increased. An effect, which could explain the observed properties of the  $Y_b(10889)$ , however without assuming an exotic nature, is *rescattering*. In the rescattering model, the decay  $\Upsilon(5S) \rightarrow \Upsilon(1S, 2S, 3S)\pi^+\pi^-$  would not proceed in a direct way, but by  $\Upsilon(5S) \rightarrow B^{(*)}\bar{B}^{(*)}$  and subsequent  $B^{(*)}\bar{B}^{(*)} \rightarrow \Upsilon(1S, 2S, 3S)\pi^+\pi^-$ . On the one hand, the peak position could be shifted upwards by the rescattering by  $+(7-20)$  MeV [50], compatible with the observed higher peak position of the  $Y_b(10889)$  compared to the  $\Upsilon(5S)$ . On the other hand, the amplitude of the rescattering is proportional to  $|\vec{p}_1|^3$ , where  $\vec{p}_1$  denotes the 3-momentum of the  $B^{(*)}$  or  $\bar{B}^{(*)}$ , and would lead to an enhancement of the observed cross section by a factor 200–600 [50]. This way this mechanism could also provide an explanation for the observed anomalous yield (see above). Quantitative predictions are however difficult, because unknown form factors [51] [50] must be assumed.

Process	$\Gamma$	$\Gamma_{e^+e^-}$	$\Gamma_{\Upsilon(1S)\pi^+\pi^-}$
$\Upsilon(2S) \rightarrow \Upsilon(1S)\pi^+\pi^-$	0.032 MeV	0.612 keV	0.0060 MeV
$\Upsilon(3S) \rightarrow \Upsilon(1S)\pi^+\pi^-$	0.020 MeV	0.443 keV	0.0009 MeV
$\Upsilon(4S) \rightarrow \Upsilon(1S)\pi^+\pi^-$	20.5 MeV	0.272 keV	0.0019 MeV
$\Upsilon(10860) \rightarrow \Upsilon(1S)\pi^+\pi^-$	110 MeV	0.31 keV	0.59 MeV

Table 4: Total widths, partial width for decay into  $e^+e^-$  and partial width for decay into  $\Upsilon(1S)\pi^+\pi^-$  for the  $\Upsilon(2S)$ ,  $\Upsilon(3S)$  and  $\Upsilon(5S)$ . The  $\Upsilon(5S)$  is denoted as  $\Upsilon(10860)$ , as it might be an admixture of several closeby states. As can be seen,  $\Gamma_{\Upsilon(1S)\pi^+\pi^-}$  is anomalously large by a factor  $>10^2$  for the  $\Upsilon(10860)$ .

## 5 A future Project: measurement of the width of the X(3872)

One of the important steps would be to measure not only the *masses* of newly observed states, but also the *widths*. As many states have natural widths in the sub-MeV regime, future experiments must be able to reach according precision. The  $\bar{\text{P}}\text{ANDA}$  experiment at FAIR (Facility for Antiproton and Ion research) at GSI Darmstadt, Germany, will be using a stored, cooled anti-proton beam. The measurement of the width of a state can be performed by a resonance scan technique. Both stochastic cooling and  $e^-$ -cooling techniques will be used, providing a momentum resolution of the antiproton beam of down to  $\Delta p/p \geq 2 \times 10^{-5}$ . The anti-protons will collide with protons in e.g. a frozen pellet target. With a maximum beam momentum of  $p \leq 15$  GeV/c, in this fixed target setup a maximum center-of-mass energy of  $\sqrt{s} \leq 5.5$  GeV can be achieved, corresponding to a very high mass of an accessible charmonium(-like) state, which would kinematically not be accessible in  $B$  meson decays or in radiative decays of  $\psi$  resonances. For momentum reconstruction, a high magnetic solenoid field of  $B=2$  T will be employed. One of the difficulties will be, that signal events (e.g. charmonium production, with subsequent decays into light mesons) and background events (hadronic production of light mesons) have very similar topologies. Thus, a hardware trigger using simple criteria, such as number of charged tracks or number of photons in the calorimeter, is not possible. Therefore  $\bar{\text{P}}\text{ANDA}$  will perform complete online reconstruction of all events with a high interaction rate of  $\leq 2 \times 10^7$ /s. The planned luminosity of  $L=2 \cdot 10^{32}$  cm $^{-2}$  s $^{-1}$  is high and would translate into a number of  $2 \cdot 10^9$   $J/\psi$  per year, if theoretically running on the  $J/\psi$  resonance only.

Cross sections in  $p\bar{p}$  formation (as an example  $\sigma(p\bar{p} \rightarrow X(3872))$ ) can be estimated from measured branching fractions (i.e.  $\mathcal{B}(X(3872) \rightarrow p\bar{p})$ ) using the principle of detailed balance, which is shown in Eq. 6.

$$\begin{aligned}
\sigma[p\bar{p} \rightarrow X(3872)] &= \sigma_{BW}[p\bar{p} \rightarrow X(3872) \rightarrow \text{all}](m_{X(3872)}) \\
&= \frac{(2J+1) \cdot 4\pi}{m_{X(3872)}^2 - 4m_p^2} \cdot \frac{\mathcal{B}(X(3872) \rightarrow p\bar{p}) \cdot \overbrace{\mathcal{B}(X(3872) \rightarrow f)}^{=1} \cdot \Gamma_{X(3872)}^2}{\underbrace{4(m_{X(3872)} - m_{X(3872)})^2}_{=0} + \Gamma_{X(3872)}^2} \\
&\stackrel{(J=1)}{=} \frac{3 \cdot 4\pi}{m_{X(3872)}^2 - 4m_p^2} \cdot \mathcal{B}(X(3872) \rightarrow p\bar{p}) . \tag{6}
\end{aligned}$$

$R$	$J$	$m$ [MeV]	$\Gamma$ [keV]	$\mathcal{B}(R \rightarrow p\bar{p})$	$\sigma(\bar{p}p \rightarrow R)$
$J/\psi$	1	$3096.916 \pm 0.011$	$92.9 \pm 2.8$	$(2.17 \pm 0.07) \times 10^{-3}$	$5.25 \pm 0.17 \mu\text{b}$
$\psi'$	1	$3686.109^{+0.12}_{-0.14}$	$304 \pm 9$	$(2.76 \pm 0.12) \times 10^{-4}$	$402 \pm 18 \text{ nb}$
$\eta_c$	0	$2981.0 \pm 1.1$	$(29.7 \pm 1.0) \times 10^3$	$(1.41 \pm 0.17) \times 10^{-3}$	$1.29 \pm 0.16 \mu\text{b}$
$\eta'_c$	0	$3638.9 \pm 1.3$	$(10 \pm 4) \times 10^3$	$(1.85 \pm 1.26) \times 10^{-4}$	$93 \pm 63 \text{ nb}$
$\chi_{c0}$	0	$3414.75 \pm 0.31$	$(10.4 \pm 0.6) \times 10^3$	$(2.23 \pm 0.13) \times 10^{-4}$	$134.1 \pm 7.8 \text{ nb}$
$h_c$	1	$3525.41 \pm 0.16$	$\leq 1 \times 10^3$	$(8.95 \pm 5.21) \times 10^{-4}$	$1.47 \pm 0.86 \mu\text{b}$
$X(3872)$	1	$3871.68 \pm 0.17$	$\leq 1.2 \times 10^3$	$\leq 5.31 \times 10^{-4}$	$\leq 68.0 \text{ nb}$

Table 5: Total spin  $J$ , mass  $m$ , width  $\Gamma$ , branching fraction for the decay into  $p\bar{p}$  and cross sections for production at  $\bar{\text{P}}\text{ANDA}$ , as derived by the principle of detailed balance for selected resonances  $R$ .

Tab. 5 summarizes cross sections for production at  $\bar{\text{P}}\text{ANDA}$  as derived by the principle of detailed balance for selected resonances  $R$ . For the  $J/\psi$ , the  $\psi'$ , the  $\eta'_c$  and the  $\chi_{c0}$  the branching fraction  $\mathcal{B}(R \rightarrow p\bar{p})$  was taken from [14]. For the  $\eta'_c$ ,  $\mathcal{B}(b \rightarrow K^+ R \rightarrow K^+ p\bar{p})$  was taken from [52] and  $\mathcal{B}(B^+ \rightarrow K^+ R)$  was taken from [14]. For the  $h_c$  and the  $X(3872)$   $\mathcal{B}(b \rightarrow K^+ R \rightarrow K^+ p\bar{p})$  was taken from [52] and the upper limit for  $\mathcal{B}(B^+ \rightarrow K^+ R)$  was taken from [14]. Typical cross sections for charmonium formation at  $\bar{\text{P}}\text{ANDA}$  are thus in the order of 10-100 nb. In the following, we assume  $\sigma(p\bar{p} \rightarrow X(3872)) = 50 \text{ nb}$ .

Detailed Monte-Carlo simulation studies of a resonance scan for  $p\bar{p} \rightarrow X(3872)$  at  $\bar{\text{P}}\text{ANDA}$  were performed. The advantage is, that in  $p\bar{p}$  collisions the  $X(3872)$  with  $J^{PC} = 1^{++}$  can be formed directly, while in  $e^+e^-$  only  $J^{PC} = 1^{--}$  is possible. The Breit-Wigner cross section for the formation and subsequent decay of a  $c\bar{c}$  resonance  $R$  of spin  $J$ , mass  $M_R$  and total width  $\Gamma_R$  formed in the reaction  $\bar{p}p \rightarrow R$  is

$$\sigma_{BW}(E_{cm}) = \frac{(2J+1)}{(2S+1)(2S+1)} \frac{4\pi(\hbar c)^2}{(E_{cm}^2 - 4(m_p c^2)^2)} \times \frac{\Gamma_R^2 \mathcal{B}R(\bar{p}p \rightarrow R) \times \mathcal{B}R(R \rightarrow f)}{(E_{cm} - M_R c^2)^2 + \Gamma_R^2/4} \tag{7}$$

where  $S$  is the spin of the (anti-)proton.

$$\sigma(E_{cm}) = \int_0^\infty \sigma_{BW}(E') G(E' - E_{cm}) dE' \tag{8}$$

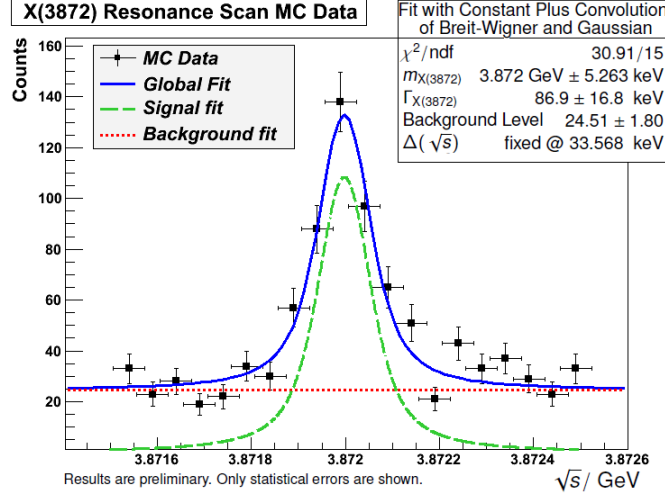


Figure 12: Final result for the simulated resonance scan of X(3872) at  $\overline{\text{PANDA}}$  with 20 scan points. For details see [55].

is a convolution of a Breit-Wigner term for the resonance and the function  $G$  for the beam resolution. If  $G$  is given by a single Gaussian distribution, then the convolution is a Voigtian distribution. The area under the resonance peak is given by

$$A = \int_0^\infty \sigma(E_{cm}) dE_{cm} = \frac{\pi}{2} \sigma_{peak} \Gamma_R \quad (9)$$

which importantly is independent of the form of  $G(E)$ .  $\sigma_{peak}$  is the cross section at  $E_{cm} = M_R c^2$  given by

$$\sigma_{peak} = \frac{(2J+1)}{(2S+1)(2S'+1)} \frac{16\pi\hbar^2 BR(\bar{p}p \rightarrow R) \times BR(R \rightarrow f)}{(M_R - 4m_p^2)c^2} \quad (10)$$

By measuring  $A$  using a fit to the excitation function and inserting  $\sigma_{peak}$  into Eq. 9, the resonance width  $\Gamma_R$  can be determined. For a complete simulation of the resonance scan, 20 simulations for  $p\bar{p} \rightarrow X(3872) \rightarrow J/\psi\pi^+\pi^-$  with background were performed for 20 beam momenta in the resonance region. The beam momenta were chosen equidistant in center-of-mass energy. For each scan point, the yield of the X(3872) was fitted by a single Gaussian. Fig. 12 shows the fitted yield as a function of  $\sqrt{s}$ . The fit was performed using a Voigtian distribution. Direct background from  $p\bar{p} \rightarrow J/\psi\pi^+\pi^-$  was taken into account as a zeroth order polynomial, although estimates [53] indicate that it is small with a cross section of 1.2 nb (i.e. a factor  $\simeq 40$  smaller than the signal). The known momentum resolution in the HESR high resolution mode was fixed as the width of the Gaussian in the convoluted Voigtian. The width of the X(3872) was reconstructed as  $\Gamma_{X(3872)} = 86.9 \pm 16.8$  keV, which is consistent with the input width of 100 keV. This simulation is a proof for the concept, and the ability of  $\overline{\text{PANDA}}$  to measure the width of a resonance in the sub-MeV regime. For additional details see [54] [55].

## 6 Summary

Recent results from  $e^+e^-$  collisions (and in particular the  $B$  meson factories) enable unique precision tests of the  $q\bar{q}$  potential in the charmonium and bottomonium region. The static potential model fails for many newly observed states (called XYZ states), indicating non- $q\bar{q}$  phenomena such as possibly tetraquark states, charmed meson molecular states or hybrid states. Future experiments such as PANDA will provide precision tests not only of masses, but also widths in the sub-MeV regime.

## 7 Acknowledgments

The author is grateful for the invitation, the hospitality in Dubna and many interesting and inspiring discussions during the school.

## References

- [1] E. Eichten, K. Gottfried, T. Kinoshita, K. D. Lane, T.-M. Yan, Phys. Rev. D17(1978)3090.
- [2] S. Godfrey, N. Isgur, Phys. Rev. D32(1985)189.
- [3] T. Barnes, S. Godfrey, E. S. Swanson, arXiv:hep-ph/0505002, Phys. Rev. D72(2005)054026.
- [4] Belle Collaboration, Nucl. Instr. Meth. A479(2002)117.
- [5] BaBar Collaboration, Nucl. Instr. Meth. A479(2002)1.
- [6] Belle Collaboration, arXiv:hep-ex/0309032, Phys. Rev. Lett. 91(2003)262001.
- [7] BaBar Collaboration, Phys. Rev. D71(2005)071103, Phys. Rev. D77(2008)111101.
- [8] CDF II Collaboration, Phys. Rev. Lett. 93(2004)072001; CDF II Collaboration, Phys. Rev. Lett. 96(2006)102002; CDF II Collaboration, Phys. Rev. Lett. 103(2009)152001.
- [9] D0 Collaboration, Phys. Rev. Lett. 93(2004)162002.
- [10] LHCb Collaboration, arXiv:1112.5310[hep-ex], Eur. Phys. J. C72(2012)1972.
- [11] CMS Collaboration, CERN-CMS-DP-2011-005; CMS Collaboration, arXiv:1302.3968[hep-ex].
- [12] Belle Collaboration, arXiv:1107.0163[hep-ex], Phys. Rev. D84(2011)052004.
- [13] N. A. Törnqvist, arXiv:hep-ph/0402237, Phys. Lett. B590(2004)209; N. A. Törnqvist, Phys. Rev. Lett. 67(1991)556.
- [14] J. Beringer et al. (Particle Data Group), Phys. Rev. D86(2012)010001.
- [15] E. Braaten, M. Lu, arXiv:0709.2697[hep-ph], Phys. Rev. D76(2007)094028; E. Braaten, M. Lu, arXiv:0710.5482[hep-ph], Phys. Rev. D77(2008)014029; E. Braaten, M. Kusunoki, arXiv:hep-ph/0412268, Phys. Rev. D69(2004)074005.
- [16] Belle Collaboration, arXiv:hep-ex/0505037.
- [17] BaBar Collaboration, arXiv:hep-ex/0607050, Phys. Rev. D74(2006)071101.
- [18] BaBar Collaboration, arXiv:hep-ex/0506081, Phys. Rev. Lett. 95(2005)142001.
- [19] CLEO-c Collaboration, arXiv:hep-ex/0611021, Phys. Rev. D74(2006)091104.
- [20] Belle Collaboration, arXiv:hep-ex/0612006.
- [21] Belle Collaboration, arXiv:0707.2541[hep-ex], Phys. Rev. Lett. 99(2007)182004.
- [22] BaBar Collaboration, arXiv:0808.1543[hep-ex].
- [23] BaBar Collaboration, arXiv:1204.2158[hep-ex], Phys. Rev. D86(2012)051102.
- [24] Belle Collaboration, arXiv:0707.3699, Phys. Rev. Lett. 99(2007)142002.
- [25] BaBar Collaboration, arXiv:hep-ex/0610057, Phys. Rev. Lett. 98(2007)212001.

- [26] F. E. Close, P. R. Page, arXiv:hep-ph/0507199, Phys. Lett. B628(2005)215.
- [27] C. Bernard, J. E. Hetrick, T. A. DeGrand, M. Wingate, C. DeTar, C. McNeile, S. Gottlieb, U. M. Heller, K. Rummukainen, B. Sugar D. Toussaint, arXiv:hep-lat/9707008, Phys. Rev. D56(1997)7039; Z.-H. Mei, X.-Q. Luo, arXiv:hep-lat/0206012, Int. J. Mod. Phys. A18(2003)5713.
- [28] Belle Collaboration, arXiv:0807.4458[hep-ex], Phys. Rev. Lett. 101(2008)172001.
- [29] BESIII Collaboration, arXiv:1303.5949[hep-ex].
- [30] Belle Collaboration, arXiv:1304.0121[hep-ex].
- [31] Belle Collaboration, arXiv:1304.3975[hep-ex], Phys. Rev. Lett. 111(2013)032001.
- [32] W. Kwong, J. L. Rosner, C. Quigg, Ann. Rev. Nucl. Part. Sci. 37(1987)325.
- [33] E. J. Eichten, K. Lane, C. Quigg, arXiv:hep-ph/0401210, Phys. Rev. D69(2004)094019.
- [34] P. Ko, J. Lee, H. S. Song, arXiv:hep-ph/9701235, Phys. Lett. B395(1997)107.
- [35] Belle Collaboration, arXiv:1103.3419[hep-ex], Phys. Rev. Lett. 108(2011)032001.
- [36] BaBar Collaboration, arXiv:1102.4565[hep-ex], Phys. Rev. D84(2011)091101(R).
- [37] D. Ebert, R.N. Faustov, V.O. Galkin, arXiv:hep-ph/0210381, Phys. Rev. D67(2003)014027.
- [38] Belle Collaboration, arXiv:1205.6351[hep-ex], Phys. Rev. Lett. 109(2012)232002.
- [39] S. Meinel, arXiv:1007.3966[hep-lat], Phys. Rev. D82(2010)114502.
- [40] A. A. Penin, arXiv:0905.4296[hep-ex].
- [41] R. J. Dowdall, B. Colquhoun, J. O. Daldrop, C. T. H. Davies, I. D. Kendall, E. Follana, T. C. Hamant, R. R. Horgan, G. P. Lepage, C. J. Monahan, E. H. Müller, arXiv:1110.6887[hep-lat], Phys. Rev. D85(2012)054509.
- [42] CLEO II Collaboration, arXiv:0805.4599[hep-ex], Phys.Rev.Lett.101(2008)182003.
- [43] BESIII Collaboration, arXiv:1002.0501, Phys.Rev.Lett.104(2010)132002.
- [44] C. Quigg, hep-ph/9707493.
- [45] Belle Collaboration, arXiv:hep-ex/0611026, Phys. Rev. D75(2007)071103.
- [46] Belle Collaboration, arXiv:0710.2577[hep-ex], Phys. Rev. Lett. 100(2008)112001.
- [47] W.-S. Hou, arXiv:hep-ph/0606016, Phys. Rev. D74(2006)017504.
- [48] Belle Collaboration, arXiv:0808.2445 [hep-ex], Phys. Rev. D82(2010)091106.
- [49] A. Ali, C. Hambrock, I. Ahmed, M. J. Aslam, arXiv:0911.2787[hep-ph], Phys. Lett. B684(2010)28; A. Ali, C. Hambrock, M. J. Aslam, arXiv:0912.5016[hep-ph], Phys. Rev. Lett. 104(2010)162001, Erratum-ibid. 107(2011)049903; A. Ali, C. Hambrock, S. Mishima, arXiv:1011.485[hep-ph], Phys. Rev. Lett. 106(2011)092002.
- [50] C. Meng, K.-T. Chao, arXiv:0805.0143[hep-ph], Phys. Rev. D78(2008)034022.
- [51] Y. A. Simonov, 0804.4635[hep-ph], JETP Lett. 87(2008)121.
- [52] LHCb collaboration, arXiv:1303.7133[hep-ex], submitted to Eur. Phys. Jour. C.
- [53] G. Y. Chen, J. P. Ma, arXiv:0802.2982[hep-ph], Phys. Rev. D77(2008)097501.
- [54] J. S. Lange, M. Galuska, Th. Geßler, W. Kühn, S. Künze, Y. Liang, D. Münchow, B. Spruck, M. Ullrich, M. Werner, arXiv:1010.2350[hep-ex].
- [55] M. Galuska *Simulation of  $X(3872)$  Decays Using the PandaRoot Framework*, Master Thesis, Justus-Liebig-Universität Giessen, 2011.